

# Bidirectional threshold switching in engineered multilayer ( $\text{Cu}_2\text{O}/\text{Ag}:\text{Cu}_2\text{O}/\text{Cu}_2\text{O}$ ) stack for cross-point selector application

Cite as: Appl. Phys. Lett. **107**, 113504 (2015); <https://doi.org/10.1063/1.4931136>

Submitted: 30 June 2015 . Accepted: 07 September 2015 . Published Online: 16 September 2015

Jeonghwan Song, Amit Prakash, Daeseok Lee, Jiyong Woo, Euijun Cha, Sangheon Lee, and Hyunsang Hwang



View Online



Export Citation



CrossMark

## ARTICLES YOU MAY BE INTERESTED IN

Threshold switching behavior of Ag-Si based selector device and hydrogen doping effect on its characteristics

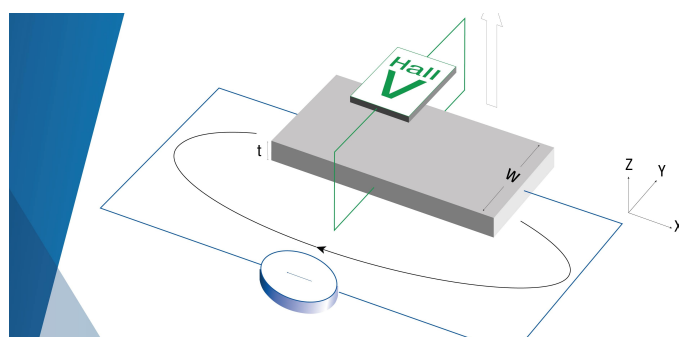
AIP Advances **5**, 127221 (2015); <https://doi.org/10.1063/1.4938548>

Bidirectional threshold switching characteristics in Ag/ $\text{ZrO}_2$ /Pt electrochemical metallization cells

AIP Advances **6**, 085316 (2016); <https://doi.org/10.1063/1.4961709>

Field-induced nucleation in threshold switching characteristics of electrochemical metallization devices

Applied Physics Letters **111**, 063109 (2017); <https://doi.org/10.1063/1.4985165>



**Tips for minimizing  
Hall measurement errors**

Download the Technical Note

**Lake Shore**  
CRYOTRONICS

# Bidirectional threshold switching in engineered multilayer (Cu<sub>2</sub>O/Ag:Cu<sub>2</sub>O/Cu<sub>2</sub>O) stack for cross-point selector application

Jeonghwan Song, Amit Prakash, Daeseok Lee, Jiyong Woo, Euijun Cha, Sangheon Lee, and Hyunsang Hwang<sup>a)</sup>

Department of Materials Science and Engineering, Pohang University of Science and Technology (POSTECH), 77 Cheongam-ro, Nam-gu, Pohang 790-784, South Korea

(Received 30 June 2015; accepted 7 September 2015; published online 16 September 2015)

In this study, we achieved bidirectional threshold switching (TS) for selector applications in a Ag-Cu<sub>2</sub>O-based programmable-metallization-cell device by engineering the stack wherein Ag was intentionally incorporated in the oxide (Cu<sub>2</sub>O) layer by a simple approach comprising co-sputtering and subsequent optimized annealing. The distribution of the Ag was directly confirmed by transmission electron microscopy and energy dispersive spectroscopy line profiling. The observed TS occurred because of the spontaneous self-rupturing of the unstable Ag filament that formed in the oxide layer. © 2015 AIP Publishing LLC. [<http://dx.doi.org/10.1063/1.4931136>]

Resistive switching memory (RRAM) is considered as a promising candidate for next generation of non-volatile memories.<sup>1</sup> Among RRAMs, programmable metallization cell (PMC) devices, also known as Conductive Bridge Random Access Memory (CBRAM), typically consist of an insulating solid electrolyte sandwiched between an electrochemically active electrode (Ag or Cu) and an inert electrode (Pt or W). The cell operation is based on the voltage-induced electrochemical formation and rupture of an Ag or Cu filament in a solid electrolyte. The PMC devices have shown excellent resistive switching properties such as large memory window, good cycle endurance, long data retention, and fast switching speed.<sup>2–4</sup>

Meanwhile, the selector device is essential to suppress the sneak current in a high-density cross-point memory array, which can lead to the failure of programming and read operations.<sup>5–11</sup> Among several types of selector devices, threshold switching (TS) devices owing to phase transition such as metal-insulator transition (MIT)<sup>9,10</sup> and ovonic TS (OTS)<sup>11</sup> were extensively investigated.

As another approach, recently, there is growing interest in adapting instability of the filament in conventional PMC devices for selector applications. When the PMC device is programmed under a lower current compliance, the small and unstable filament is formed. Accordingly, the spontaneous self-rupturing of the unstable filament occurred when the applied bias is removed, which can be used as a TS device. However, previously reported TS property in PMC device was solely limited for unipolar selector applications because the filament source was provided from only one-side of active electrode.<sup>12–14</sup> Therefore, the finite source for unstable filament should be supplied from the both side of the electrodes for bi-polar selector applications.

In this study, we proposed an engineered multilayer stack showing bidirectional TS behavior. A finite source layer of Ag was inserted in-between the electrolyte by using co-sputtering. After performing the optimized annealing,

which enhanced the Ag diffusion, the stack exhibited bidirectional TS with a sharp ON/OFF transition. The incorporation of Ag into the electrolyte acting as a source for filament formation under both positive- and negative-bias applications was confirmed by Transmission electron microscopy (TEM) and energy dispersive spectroscopy (EDS) line profiling analyses.

For this work, we adopted cuprous oxide (Cu<sub>2</sub>O) as an electrolyte. The Cu<sub>2</sub>O is abundantly available, nontoxic in nature, has low cost of production and it has been extensively studied for various applications such as resistive switching memories, solar cells, spintronics, gas sensors, and photocatalysis.<sup>15</sup> The Cu<sub>2</sub>O films can be prepared using various deposition techniques such as electrodeposition, thermal oxidation, chemical vapor deposition, reactive sputtering, radical oxidation, and RF sputtering.<sup>16–20</sup> Among these techniques, the Cu<sub>2</sub>O films which were used in this work were deposited using Cu<sub>2</sub>O (2 in. diameters, 99.9%, LTS Chemical, USA) target and argon gas with RF magnetron sputtering.

We fabricated Ag-Cu<sub>2</sub>O-based PMC devices using a 250-nm via-hole structure. For the isolation layer, a 100-nm-thick SiO<sub>2</sub> layer was deposited on a Pt bottom electrode (BE) substrate by plasma-enhanced chemical vapor deposition. Subsequently, 250-nm via-holes were defined by lithographic and reactive-ion etching processes in a sequence.<sup>21</sup> Three types of samples—having structures of Ag/Cu<sub>2</sub>O/Pt, Pt/Ag:Cu<sub>2</sub>O/Pt, and Pt/Cu<sub>2</sub>O/Ag:Cu<sub>2</sub>O/Cu<sub>2</sub>O/Pt—were prepared and investigated. For the Ag/Cu<sub>2</sub>O/Pt sample, a 20-nm-thick Cu<sub>2</sub>O layer was deposited by RF sputtering using a Cu<sub>2</sub>O target with an RF power of 100 W. Then, as a top electrode (TE), Ag was deposited by direct-current (DC) sputtering using an Ag target and a DC power of 100 W. For the Pt/Ag:Cu<sub>2</sub>O/Pt sample, a 20-nm-thick Ag:Cu<sub>2</sub>O layer was co-sputter-deposited using Cu<sub>2</sub>O and Ag targets with powers of 100 and 10 W, respectively. To fabricate the Pt/Cu<sub>2</sub>O/Ag:Cu<sub>2</sub>O/Cu<sub>2</sub>O/Pt sample, a 5-nm-thick Ag:Cu<sub>2</sub>O layer co-sputter-deposited under the previously described conditions was sandwiched between two 10-nm-thick Cu<sub>2</sub>O layers deposited by RF sputtering using a Cu<sub>2</sub>O target and an RF power of 100 W. In both the stacks, Pt TE was deposited by

<sup>a)</sup> Author to whom correspondence should be addressed. Electronic mail: [hwanghs@postech.ac.kr](mailto:hwanghs@postech.ac.kr)

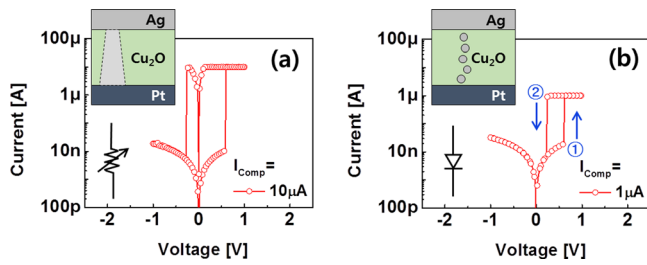


FIG. 1. Compliance current-dependent (a) MS and (b) TS behaviors and schematics for Ag/Cu<sub>2</sub>O/Pt stack PMC device.

DC sputtering with a DC power of 100 W. Physical analyses were performed by TEM and EDS line profiling. Electrical characterizations were conducted using a semiconductor parameter analyzer (Agilent B1500). Voltage bias was applied on the TE while the BE was kept at electrical ground.

The PMC device with the Ag/Cu<sub>2</sub>O/Pt structure exhibits conventional non-volatile memory switching (MS) and volatile TS at a high ( $>10 \mu\text{A}$ ) and low ( $<1 \mu\text{A}$ ) current compliance ( $I_{\text{comp}}$ ), respectively (Fig. 1). Fig. 1(a) shows the current–voltage (I–V) characteristics of the MS at an  $I_{\text{comp}}$  of  $10 \mu\text{A}$ . As the bias voltage was swept to a positive polarity, the cell resistance abruptly decreased from a high-resistance state (HRS) to a low-resistance state (LRS) at  $+0.6 \text{ V}$ , which corresponds to the SET operation. Because of the thicker filament formation, this LRS was stable even after the removal of the applied voltage, as schematically shown in the inset of Fig. 1(a). When the applied voltage was swept to a negative bias after the SET operation, the resistance switched abruptly from the LRS to the HRS at  $-0.3 \text{ V}$  owing to the filament rupture, which corresponds to the RESET operation. In contrast, the device exhibited the TS behavior at a smaller  $I_{\text{comp}}$  of  $1 \mu\text{A}$ , as shown in Fig. 1(b). When the voltage swept past a certain voltage called the threshold voltage ( $V_{\text{th}} = +0.6 \text{ V}$ ), the current abruptly increased to  $I_{\text{comp}}$  ( $1 \mu\text{A}$ ), and the device switched to the ON state. However, when the sweep voltage reached a certain value ( $0.2 \text{ V}$ ) during the backward sweep, the device did not remain in the ON state, and the current decreased to the initial high-resistance level, exhibiting typical TS behavior. This TS can be understood as the spontaneous self-rupturing of the unstable Ag filament in the Cu<sub>2</sub>O layer, as shown in the inset of Fig. 1(b).<sup>12</sup> However, because the filament source was provided from only one-side of active electrode, the TS in the Ag/Cu<sub>2</sub>O/Pt stack shows unipolar characteristics and it was solely limited for unipolar selector applications.

Therefore, to obtain a bidirectional TS characteristics for bi-polar selector applications, we proposed Ag-doped

Cu<sub>2</sub>O (Ag:Cu<sub>2</sub>O) as a switching layer deposited by a simple co-sputtering method. With the Ag:Cu<sub>2</sub>O switching layer, the device was expected to exhibit the bidirectional TS behavior because the Ag source can be supplied from inside of the electrolyte for filament formation under both positive and negative-bias applications. However, as shown in Fig. 2(a), the Pt/Ag:Cu<sub>2</sub>O/Pt stacked device exhibits metallic behavior because of the excess amount of Ag source present in the Cu<sub>2</sub>O layer, even though the Ag:Cu<sub>2</sub>O layer was deposited with the smallest possible Ag deposition-rate conditions. For this reason, to minimize the Ag concentration in the electrolyte, we utilized a multi-layer structure in which the Ag:Cu<sub>2</sub>O layer was sandwiched between two insulating undoped Cu<sub>2</sub>O layers. The I–V curve of the resulting device, which had a Pt/Cu<sub>2</sub>O/Ag:Cu<sub>2</sub>O/Cu<sub>2</sub>O/Pt structure, is shown in Fig. 2(b). The device still did not exhibit any switching characteristics, and it behaved like an insulator as the current remained very low throughout the bias application. The insulating behavior can be understood as the failure of the filament formation in the undoped Cu<sub>2</sub>O layers because the cell resistance was similar with that of HRS in Ag/Cu<sub>2</sub>O/Pt stack (Fig. 1) which has no Ag filament. To overcome this problem by enhancing the Ag diffusion into the undoped Cu<sub>2</sub>O layers, we performed annealing at various temperatures: 100, 200, and 350 °C. Fig. 3 summarizes the I–V curves obtained from the devices after annealing. The device annealed at 200 °C exhibited bidirectional TS, as shown in Fig. 2(c). On the other hand, the device annealed at 100 °C exhibited insulating characteristics and metallic behavior when annealed at 350 °C. This behavior is attributed to the amount of the Ag source in the case of the annealing at 100 °C, which was insufficient for the Ag diffusion and excess Ag diffusion at the annealing temperature of 350 °C. In addition, the results indicate that the proper control of the Ag diffusion is crucial to obtain the bidirectional TS.

To confirm the proposed mechanism, the distribution of the Ag source was directly confirmed by TEM images and EDS line profiling, as shown in Fig. 4. Figs. 4(a)–4(c) show the uniformly distributed Ag source over the entire Ag:Cu<sub>2</sub>O electrolyte, which caused the metallic behavior (Fig. 2(a)). On the other hand, the Ag was sharply distributed in the multi-layer structure having the Ag:Cu<sub>2</sub>O layer between two insulating undoped Cu<sub>2</sub>O layers, as shown in Figs. 4(d)–4(f). In this case, as previously discussed, the Ag source was not available to form the filament from the BE to the TE, which agrees well with the results of Fig. 2(b). Finally, after annealing at 200 °C, the bidirectional TS characteristics of the

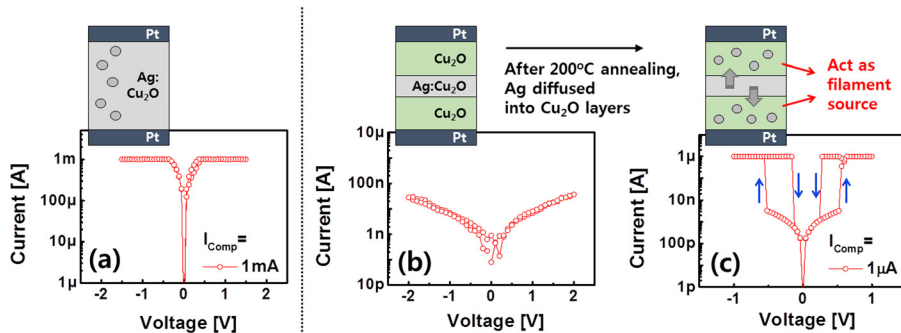


FIG. 2. I–V characteristics and schematics for (a) Pt/Ag:Cu<sub>2</sub>O/Pt stack device and (b) and (c) Pt/Cu<sub>2</sub>O/Ag:Cu<sub>2</sub>O/Cu<sub>2</sub>O/Pt stack device; (c) results for Pt/Cu<sub>2</sub>O/Ag:Cu<sub>2</sub>O/Cu<sub>2</sub>O/Pt stack device after annealing at 200 °C.

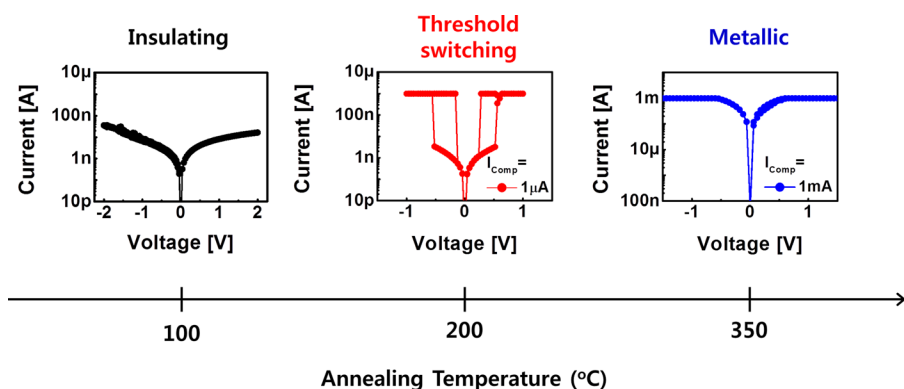


FIG. 3. Comparison of the I–V characteristics of the Pt/Cu<sub>2</sub>O/Ag:Cu<sub>2</sub>O/Cu<sub>2</sub>O/Pt stack samples annealed at 100, 200, and 350 °C.

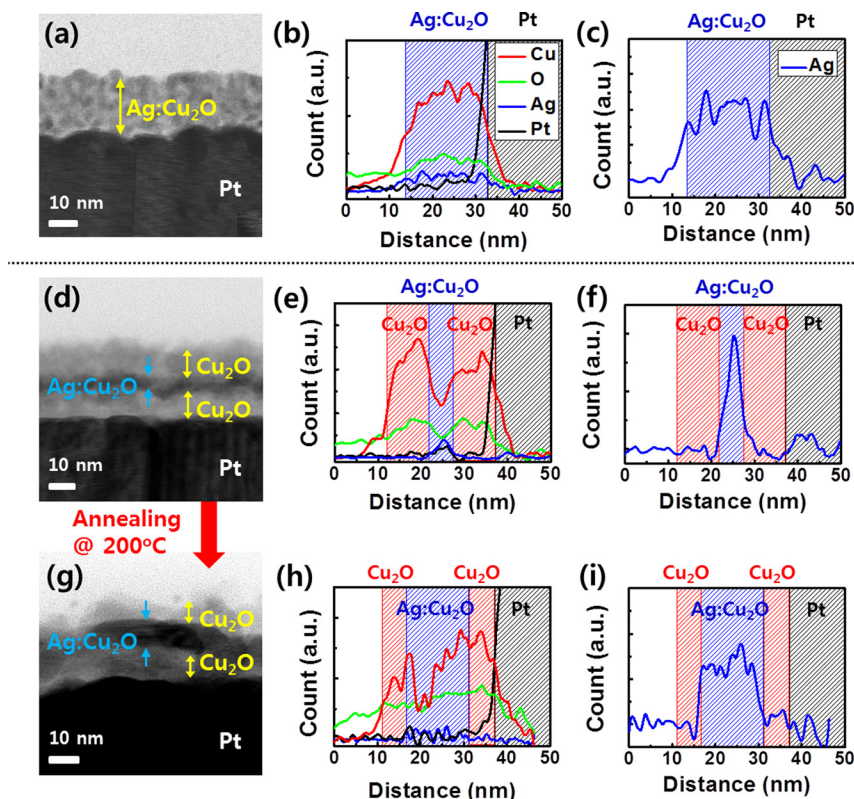


FIG. 4. TEM images and corresponding plots of the EDS line profiles of (a)–(c) the Ag:Cu<sub>2</sub>O stack and (d)–(i) the Cu<sub>2</sub>O/Ag:Cu<sub>2</sub>O/Cu<sub>2</sub>O stack. (g)–(i) show the results for the Cu<sub>2</sub>O/Ag:Cu<sub>2</sub>O/Cu<sub>2</sub>O-stack device after annealing at 200 °C. Among the EDS line-profiling curves, (b), (e), and (h) correspond to the whole element, and (c), (f), and (i) correspond only to the Ag element.

multi-layer structured device were confirmed by TEM and EDS line profiling, as shown in Figs. 4(g)–4(i). Clearly, the Ag distribution was broadened after the annealing. This means that the Ag source diffused from the Ag:Cu<sub>2</sub>O layer into the undoped Cu<sub>2</sub>O layers after the annealing process at 200 °C. This result agrees well with the results of Fig. 2(c).

We investigated the TS characteristics of a PMC device having Cu<sub>2</sub>O as an electrolyte and Ag as an electrochemically active electrode. The TS occurred because of the spontaneous self-rupturing of the unstable Ag filament in the Cu<sub>2</sub>O layer. According to our in-depth analysis and understanding of the switching mechanism of TS devices, we propose a multilayer (Cu<sub>2</sub>O/Ag:Cu<sub>2</sub>O/Cu<sub>2</sub>O) stack to obtain bidirectional TS for bipolar selector applications. The introduced Ag:Cu<sub>2</sub>O source layer in-between the electrolyte and optimal annealing conditions were found to be crucial for achieving the bidirectional TS. The Ag:Cu<sub>2</sub>O layer can supply the Ag source into both side of the electrodes and the optimal annealing conditions can control the amount of diffused Ag source for unstable filament formation under both

positive- and negative-bias applications. The Ag diffusion was also directly confirmed by using TEM and EDS line-profiling analyses. Our research can be applicable to other PMC devices also, and provides an approach for achieving bidirectional TS characteristics for bipolar selector applications. We expect that the material optimization based on the deeper understanding of the interaction between the filament and the surrounding electrolyte can further improve its selector performances for realization of high-density cross-point memory array.

This work was supported by the POSTECH-Samsung Electronics ReRAM Cluster Research.

<sup>1</sup>R. Waser and M. Aono, “Nanoionics-based resistive switching memories,” *Nat. Mater.* **6**, 833–840 (2007).

<sup>2</sup>I. Valov, R. Waser, J. R. Jameson, and M. N. Kozicki, “Electrochemical metallization memories—fundamentals, applications, prospects,” *Nanotechnology* **22**(25), 254003 (2011).

<sup>3</sup>S. Peng, F. Zhuge, X. Chen, X. Zhu, B. Hu, L. Pan, B. Chen, and R. W. Li, “Mechanism for resistive switching in an oxide-based electrochemical metallization memory,” *Appl. Phys. Lett.* **100**, 072101 (2012).

- <sup>4</sup>Y. Liu, P. Gao, X. Jiang, K. Bi, H. Xu, and W. Peng, "Percolation network in resistive switching devices with the structure of silver/amorphous silicon/p-type silicon," *Appl. Phys. Lett.* **104**, 043502 (2014).
- <sup>5</sup>M. J. Lee, Y. Park, B. S. Kang, S. E. Ahn, C. Lee, K. Kim, W. Xianyu, G. Stenfanovich, J. H. Lee, S. J. Chung, Y. H. Kim, C. S. Lee, J. B. Park, I. G. Baek, and I. K. Yoo, "2-stack 1D-1R cross-point structure with oxide diodes as switch elements for high density resistance RAM applications," in *Proceedings of IEEE Electron Device Meeting* (2007), pp. 771–774.
- <sup>6</sup>K. Virwani, G. W. Burr, R. S. Shenoy, C. T. Rettner, A. Padilla, T. Topuria, P. M. Rice, G. Ho, R. S. King, K. Nguyen, A. N. Bowers, M. Jurich, M. BrightSky, E. A. Joseph, A. J. Kellock, N. Arellano, B. N. Kurdi, and K. Gopalakrishnan, "Sub-30 nm scaling and high-speed operation of fully-confined access-devices for 3D crosspoint memory based on mixed-Ionic-electronic-conduction (MIEC) materials," in *Proceedings of IEEE International Electron Device Meeting* (2012), pp. 2.7.1–2.7.4.
- <sup>7</sup>A. Kawahara, R. Azuma, Y. Ikeda, K. Kawai, Y. Katoh, K. Tanabe, T. Nakamura, Y. Sumimoto, N. Yamada, N. Nakai, S. Sakamoto, Y. Kayakawa, K. Tsuji, S. Yoneda, A. Himeno, K. I. Origasa, K. Shimakawa, T. Takagi, T. Mikawa, and K. Aono, "An 8 Mb multi-layered cross-point ReRAM macro with 443 MB/s write throughput," *IEEE ISSCC Tech. Dig. Pap.* **2012**, 432–434.
- <sup>8</sup>V. S. S. Srinivasan, S. Chopra, P. Karakare, P. Bafna, S. Lashkare, P. Kumbhare, Y. Kim, S. Srinivasan, S. Kuppurao, S. Lodha, and U. Ganguly, "Punchthrough-diode-based bipolar RRAM selector by Si epitaxy," *IEEE Electron Device Lett.* **33**(10), 1396–1398 (2012).
- <sup>9</sup>W. G. Kim, H. M. Lee, B. Y. Kim, K. H. Jung, T. G. Seong, S. Kim, H. C. Jung, H. J. Kim, J. H. Yoo, H. D. Lee, S. G. Kim, S. Chung, K. J. Lee, J. H. Lee, H. S. Kim, S. H. Lee, J. Yang, Y. Jeong, and R. S. Williams, "NbO<sub>2</sub>-based low power and cost effective 1S1R switching for high density cross point ReRAM application," *Symp. VLSI Technol., Dig. Tech. Pap.* **2014**, pp. 138–139.
- <sup>10</sup>D. Lee, J. Park, S. Park, J. Woo, K. Moon, E. Cha, S. Lee, J. Song, Y. Koo, and H. Hwang, "BEOL compatible (300 °C) TiN/TiO<sub>x</sub>/Ta/TiN 3D nanoscale (~10 nm) IMT selector," in *Proceedings of IEEE International Electron Device Meeting (IEDM)* (2013), pp. 10.7.1–10.7.4.
- <sup>11</sup>S. Kim, Y. B. Kim, K. M. Kim, S. J. Kim, S. R. Lee, M. Chang, E. Cho, M. J. Lee, D. Lee, C. J. Kim, U. I. Chung, and I. K. Yoo, "Performance of threshold switching in chalcogenide glass for 3D stackable selector," in *Proceedings of Symposium on VLSI Technology* (2013), pp. T240–T241.
- <sup>12</sup>J. V. D. Hurk, E. Linn, H. Zhang, R. Waser, and I. Valov, "Volatile resistance states in electrochemical metallization cells enabling non-destructive readout of complementary resistive switches," *Nanotechnology* **25**(42), 425202 (2014).
- <sup>13</sup>S. Ambrogio, S. Balatti, S. Choi, and D. Ielmini, "Impact of the mechanical stress on switching characteristics of electrochemical resistive memory," *Adv. Mater.* **26**, 3885 (2014).
- <sup>14</sup>H. Wang, Y. Du, Y. Li, B. Zhu, W. R. Leow, Y. Li, J. Pan, T. Wu, and X. Chen, "Configurable resistive switching between memory and threshold characteristics for protein-based devices," *Adv. Funct. Mater.* **25**, 3825–3831 (2015).
- <sup>15</sup>H. M. Jing, Z. M. Yu, and L. J. Li, "Antibacterial properties and corrosion resistance of Cu and Ag/Cu porous materials," *J. Biomed. Mater. Res., Part A* **87A**, 33 (2008).
- <sup>16</sup>A. E. Rakhshani, "Preparation, characteristics and photovoltaic properties of cuprous oxide—A review," *Solid-State Electron.* **29**, 7 (1986).
- <sup>17</sup>S. H. Jeong and E. S. Aydil, "Heteroepitaxial growth of Cu<sub>2</sub>O thin film on ZnO by metal organic chemical vapor deposition," *J. Cryst. Growth* **311**(17), 4188–4192 (2009).
- <sup>18</sup>Z. Zang, A. Nakamura, and J. Temmyo, "Nitrogen doping in cuprous oxide films synthesized by radical oxidation at low temperature," *Mater. Lett.* **92**, 188 (2013).
- <sup>19</sup>Z. Zang, A. Nakamura, and J. Temmyo, "Single cuprous oxide films synthesized by radical oxidation at low temperature for PV application," *Opt. Express* **21**, 11448 (2013).
- <sup>20</sup>W. Y. Yang, W. G. Kim, and S. W. Rhee, "Radio frequency sputter deposition of single phase cuprous oxide using Cu<sub>2</sub>O as a target material and its resistive switching properties," *Thin Solid Films* **517**, 967 (2008).
- <sup>21</sup>J. Lee, J. Shin, D. Lee, W. Lee, S. Jung, M. Jo, J. Park, K. P. Biju, S. Kim, S. Park, and H. Hwang, "Diode-less nano-scale ZrO<sub>x</sub>/HfO<sub>x</sub> RRAM device with excellent switching uniformity and reliability for high-density cross-point memory applications," in *Proceedings of IEEE International Electron Device Meeting (IEDM)* (2010), pp. 19.5.1–10.7.4.